Multidisciplinary | Rapid Review | Open Access Journal

COMMUNICATIONS, APPLICATIONS, CONTROL AND MODELLING

Received February 22, 2018, accepted April 4, 2018, date of publication April 13, 2018, date of current version May 9, 2018.

Digital Object Identifier 10.1109/ACCESS.2018.2826650

Non-Orthogonal Multiple Access for Unmanned Aerial Vehicle Assisted Communication

MUHAMMAD FARHAN SOHAIL[1,2], (Student Member, IEEE), CHEE YEN LEOW[1], (Member, IEEE), AND SEUNGHWAN WON[3], (Senior Member, IEEE)

[1]Wireless Communication Centre, Faculty of Electrical Engineering, Universiti Teknologi Malaysia, Johor 81310, Malaysia
[2]Department of Electrical Engineering, National University of Modern Languages, Islamabad 44000, Pakistan
[3]School of Electronics and Computer Science, University of Southampton Malaysia Campus, Johor 79200, Malaysia

Corresponding author: Chee Yen Leow (bruceleow@fke.utm.my)

This work was supported in part by H2020-MSCA-RISE-2015 under Grant 690750, in part by the Ministry of Higher Education Malaysia under Grant 4F818, Grant 07085, Grant 4J210, and in part by Universiti Teknologi Malaysia under Grant 19H58.

ABSTRACT The future wireless networks promise to provide ubiquitous connectivity to a multitude of devices with diversified traffic patterns wherever and whenever needed. For the sake of boosting resilience against faults, natural disasters, and unexpected traffic, the unmanned aerial vehicle (UAV)-assisted wireless communication systems can provide a unique opportunity to cater for such demands in a timely fashion without relying on the overly engineered cellular network. However, for UAV-assisted communication, issues of capacity, coverage, and energy efficiency are considered of paramount importance. The case of non-orthogonal multiple access (NOMA) is investigated for aerial base station (BS). NOMA's viability is established by formulating the sum-rate problem constituting a function of power allocation and UAV altitude. The optimization problem is constrained to meet individual user-rates arisen by orthogonal multiple access (OMA) bringing it at par with NOMA. The relationship between energy efficiency and altitude of a UAV inspires the solution to the aforementioned problem considering two cases, namely, altitude fixed NOMA and altitude optimized NOMA. The latter allows exploiting the extra degrees of freedom of UAV-BS mobility to enhance the spectral efficiency and the energy efficiency. Hence, it saves joules in the operational cost of the UAV. Finally, a constrained coverage expansion methodology, facilitated by NOMA user rate gain is also proposed. Results are presented for various environment settings to conclude NOMA manifesting better performance in terms of sum-rate, coverage, and energy efficiency.

INDEX TERMS Non-orthogonal multiple access (NOMA), orthogonal multiple access (OMA), unmanned aerial vehicle (UAV), sum-rate maximization, coverage maximization, aerial cells, energy efficiency.

I. INTRODUCTION

Lately, Unmanned Aerial Vehicle (UAV) assisted mobile communication systems have been in the limelight for several deployment scenarios [1]–[3]. UAVs can be instrumental in supporting the terrestrial wireless network by acting as a UAV Base Station (UAV-BS) to handle short-term erratic traffic demand in hotspots such as sports event as well as a concert or to mitigate congestion through data off-loading in access network [2]. They can provide means to swiftly deploy recovery networks to connect first responder personnel in cases of natural calamity when the terrestrial network is partially or entirely malfunctioning [1] or function as capacity and coverage enhancing relaying nodes and so on [3]. It is conceivable that the UAV will provide additional support as either a stand-alone aerial BS [4]–[6] or as a part of a heterogeneous network with the possibility of a multi-tier airborne cellular network [2]. Irrespective of the deployment scenario, the inherited flexibility of UAV-assisted communication systems in terms of better channel conditions guaranteeing Line-of-Sight (LOS) links, faster deployment, and maneuverability to find its parameters such as the best possible set of position and altitude to achieve better communication links with connected devices, can cater for the ever-rising diversified traffic demands whenever and wherever required.

The fruitful deployment of UAV based communication systems for 5G and beyond future wireless networks is highly involved in finding joint solutions to challenge of ubiquitous connectivity with both a multitude of devices in a spectral efficient way as well as with energy-efficient transmission

and operation of the UAV-BS for maximized and harmonized coverage and capacity [7], [8]. It should be noted that suitable energy efficiency for the UAV-assisted communication system achieves paramount importance in the overall performance of the system. Efficient energy consumption results in enhanced airtime for the communication system, improving bits/Joules for a given energy level. Furthermore, coverage and capacity of an aerial cell are attributed to many factors such as the transmission power, antenna gains, UAV altitude, deployment environment, and prominently radio access technology [2].

Recently, power domain NOMA reputations have climbed sharply as a fundamental solution to the challenges encompassing the next generation wireless networks [9]–[16]. NOMA has been proved to exhibit improved spectral efficiency, balanced and fair access as compared to OMA technologies [15], [16], with the ability to cater for multiple devices in the same frequency, time, or code resource thus providing efficient access to massive connected devices [9], [11]. Furthermore, NOMA is also instrumental in reducing the interference by employing orthogonal resources as in Orthogonal Frequency Division Multiple Access (OFDMA) [17] or by sharing a single beam between multiple users for intra-cluster access and using NOMA for inter-cluster access [18].

Current studies have focused on provisioning Air to Ground (A2G) communication services mainly through placement optimization under various viewpoints [7], [19], [20]. Work presented in [20], considered a single UAV deployment scenario having zero interference to study optimal UAV altitude for maximized coverage. Mozaffari *et al.* [7] worked with both single and multiple UAV deployment scenarios as well as examined optimum altitude and separation between interfering UAVs. The performance of UAV based communication systems has also been addressed in [19] for the underlaid Device to Device (D2D) deployment scenario. This work assumed interference raised by D2D network nodes, without considering the presence of terrestrial BS. Additionally, there have been a few studies discussing the performance of NOMA for UAV based communication system [21], [22]. A NOMA enabled fixed-wing UAV deployment was proposed in [21] to support coverage for ground users situated outside BS offloaded location. Sharma and Kim [21] also suggested a multiple access mode selection (NOMA/OMA) based on conditions guaranteeing better outage probability for the ground users. An analysis of bit allocation and trajectory optimization for UAV mounted cloudlet for off-loading application was performed in [22], where NOMA demonstrated better energy conservation for the mobile users. In contrast to [21] and [22], this paper discusses a rather typical deployment scenario of an aerial BS, where the aspects of coverage and capacity are addressed considering performance thresholds for both cell-edge as well as the cell-center users. Furthermore, the implications of UAV altitude on coverage, capacity, and energy consumption considering different multiple access techniques that have been ignored in the literature also need to be addressed.

Thus, for a prolific deployment of UAV based communication systems, it is imperative to compare the performance of NOMA for UAV based communication systems to one based on OMA, in terms of optimized deployment, resource dispersal, performance, and energy efficiency. The main contributions of the paper are as follows:

1) This paper proposes a power allocation scheme to maximize the sum-rate of the communication system with reducing energy expense for the UAV. The optimization problem is formulated as a function of the altitude of the UAV-BS, constrained to meet or exceed the individual user-rates set forth by OMA for the same deployment scenario and target area. Energy models in literature are discussed and the relationship between UAV altitude and its energy efficiency is presented.
2) Furthermore, a methodology is proposed to render expansion of the aerial cell coverage, which is facilitated by NOMA user-rate gains. Average rate and coverage under constraint is used as a tool to analyze the performance of the proposed schemes. Analytical and numerical analyses are presented for the proposed schemes and performance comparisons are also provided with altitude fixed OMA and NOMA schemes.
3) Results are presented for various target regions and deployment environments i.e., rural, urban, and dense-urban. Clearly, the proposed scheme achieves better sum-rate at a lower altitude which reduces the overall energy expenditure of the UAV. The findings are capable of guaranteeing more flight time and increasing bits/joule ratio.

The remainder of the paper is organized as follows. Section II briefly describes the system model and the channel model. In Section III, some existing energy models are analyzed. Section IV examines the performance of OMA at the optimal altitude. Methodology to maximize NOMA performance are presented in Section V. Section VI illustrates the simulation results, and our conclusions are finally drawn in Section VII.

II. SYSTEM AND CHANNEL MODEL

In this section the system model and A2G channel model are discussed.

A. SYSTEM MODEL

Consider a quasi-stationary low altitude rotary-wing UAV-BS deployed to provide wireless coverage in a disc-shaped circular region with a radius of Rc meters, where the radius of the cell is determined by the cell-edge user. Fig. 1 represents a UAV-BS deployment scenario for two users located at points R and S, respectively, whereas the UAV-BS is hovering at altitude of H meters above the ground level, considered in the center of the target region, depicted by point P in Fig. 1. The vertical projection of the UAV-BS is represented by Q point. The distance between point Q and

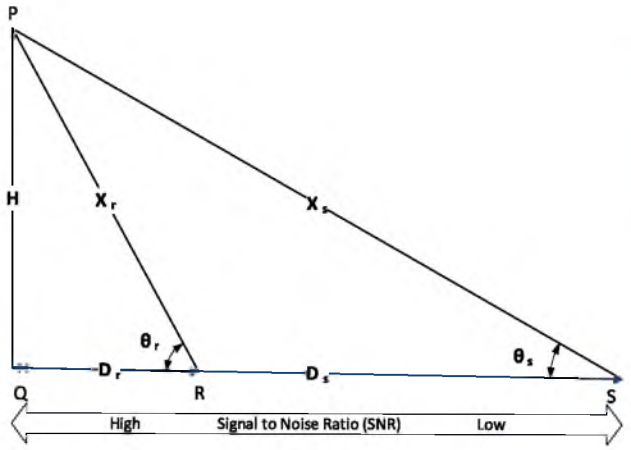

FIGURE 1. System model: A two-user UAV-assisted communication system, where PR and PS define the UAV-user links.

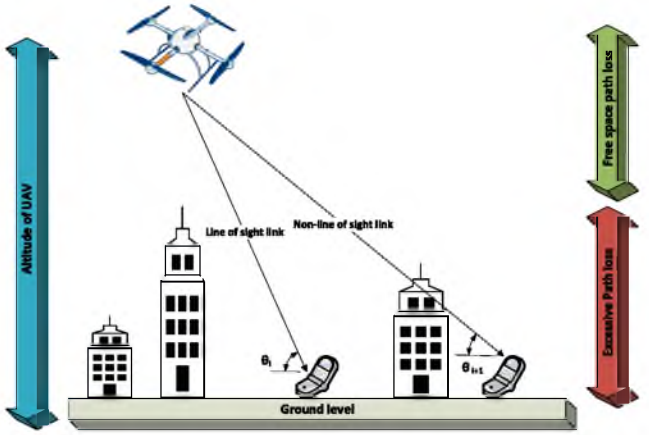

FIGURE 2. Excessive path loss model.

each user is represented by D_j. Then, the distance between the UAV-BS and each user is computed as:

$$X_j = \sqrt{D_j^2 + H^2}, \quad j \in \{r, s\}. \tag{1}$$

The elevation angle of UAV-BS with respect to each user is defined as:

$$\theta_j = \arctan(\frac{H}{D_j}), \quad j \in \{r, s\}. \tag{2}$$

B. CHANNEL MODEL

Based on widely-adopted A2G channel model in the literature [5]–[7], [19], the users can be classified as having either LOS link or strong Non-Line-Of-Sight (NLOS) link with UAV-BS [23]. This classification is based on probabilistic model which depends on the environmental profile mainly defined by density and height of buildings in the coverage region as well as the relative distance between the user and UAV together, which defines the elevation angle. The effect of small scale fading is ignored in this model as probability of occurrence of weak multi-paths is much less than that of having LOS link or strong NLOS link [24]. The probability of a user experiencing a LOS link with UAV-BS is expressed by [23]:

$$Pr_j(LOS) = \frac{1}{1 + \alpha \exp(-\beta[\theta_j - \alpha])}, \tag{3}$$

where α and β are constant values relating to the environmental profile of the coverage region such as rural, sub-urban, dense urban etc. The probability of user experiencing NLOS links is computed as:

$$Pr_j(NLOS) = 1 - Pr_j(LOS). \tag{4}$$

The $\Pr_j(LOS)$ is an increasing function of the elevation angle and thus increasing the altitude of the UAV creates an opportunity for the ground user to have unobstructed LOS link with the UAV-BS. As presented in Fig. 2, the link between UAV and the ground users constitutes two distinctive scattering environments, namely low scattering and reflection close to the UAV as well as high scattering due to presence of man-made structures close to the ground users. Considering this fact, the total path loss is computed by free space path loss and excessive loss having higher value for NLOS links compared to LOS links due to excessive losses caused by reflection of the transmitted signals and shadowing which is contributed by objects obstructing the paths in the coverage region.

Thus, considering the Downlink (DL) transmission, the received power by *j th* user is given as [23]:

$$P_{rx,j}(dB) = P_{tx}(dB) - L_j(dB), \tag{5}$$

where P_{tx} represents the transmitted power by the UAV-BS and L_j indicates the path loss for A2G channel between the UAV-BS and the *j th* user on the ground, computed as [19]:

$$L_j = \begin{cases} 10\eta \log(X_j) + \varkappa_{LOS}, & LOS\ link \\ 10\eta \log(X_j) + \varkappa_{NLOS}, & NLOS\ link, \end{cases} \tag{6}$$

where η denotes the path loss exponent. $\varkappa_{LOS}$ and $\varkappa_{NLOS}$ represent the excessive path losses of both LOS and NLOS links owing to shadow fades, respectively. Both terms comply with normal distribution, whose mean and variance are dependent on the elevation angle and environment dependent constant values [23]. Typically, the knowledge of UAV and user location without having terrain map cannot warrant information about the type of link (LOS/NLOS) between the UAV and the user. Thus, the relationship in (5) is rewritten as $P_{rx,j}(dB) = P_{tx}(dB) - \overline{L_j}(R_c, H)$, where $\overline{L_j}(R_c, H)$ defines the mean path loss considering probabilities for both LOS and NLOS UAV-user links computed as [7]:

$$\overline{L_j}(R_c, H) = Pr_j(LOS)L_j(LOS) + Pr_j(NLOS)L_j(NLOS) \tag{7}$$

III. ENERGY MODEL

Zorbas *et al.* [25] drew an explicit relationship associating the energy consumption of rotary-wing UAV with its altitude and weight. According to the suggested model, the energy

consumption of UAV at any time T can be given as $E_T = mgH$, where mg is determined by the weight of the UAV m and acceleration of gravity g as well as H represents the altitude of the UAV at time T. The relationship between the altitude of UAV and its energy consumption has also been reported and proven through experiments in [26]–[28]. However, the model presented in [25] is simplistic and falls well short of acknowledging many factors affecting the overall energy consumption such as velocity, flight maneuvers, motor and blade profiles, etc. Ueyama *et al.* [27] and Franco and Buttazzo [28] also presented real measured data for different postures of the UAV i.e. idling on the ground, ascending to and descending from a certain altitude, hovering, and moving in a straight flight. Based on the results, energy consumption increases dramatically to reach higher altitudes and hovering which usually consumes less energy among other maneuvers of the UAV, is also related to the hovering altitude. The total energy consumption of a UAV to reach a desired altitude H from the initial ground position and perform hovering for time t can be given as [28]:

$$E = E_{climb} + E_{hover} \tag{8}$$

$$= P_{climb}\frac{H}{v_{climb}} + P_{hover}t, \tag{9}$$

where, P_{climb} and P_{hover} represent the power required by the UAV to climb and hover, respectively. Also, the velocity of ascending is denoted as v_{climb} and t represents the flight duration. The relationship presented in (9) can be further elaborated based on the work presented by the authors in [29] suggesting that the UAV may attain high altitude for better coverage, by contrast with fixed wing UAV. This also leads to more energy consumption. The energy consumption model given in (9) can be rewritten as [29]:

$$E = \underbrace{P_{max}(\frac{H}{v_{climb}})}_{P_{climb}} + \underbrace{(\psi + \Gamma H)}_{P_{hover}}t, \tag{10}$$

where ψ represents the minimum power needed to hover just over the ground, Γ denotes the motor speed multiplier, P_{max} means the maximum power of the motor. The terms ψ and Γ depend on UAV weight and the characteristics of the motor, respectively. Energy consumption needed to lift UAV to an altitude H with velocity v_{climb} is $P_{max}(\frac{H}{v_{climb}})$. Assuming optimized velocity for a given UAV design, a reduction in the operational altitude of the UAV allows further energy savings. Specifically, let H_O be the optimized altitude for the UAV given OMA (detailed in Section IV). Then, the energy consumption E_O assuming OMA can be written as:

$$E_O = P_{max}(\frac{H_O}{v_{climb}}) + (\psi + \Gamma H_O)t. \tag{11}$$

Similarly, E_N defines the operational energy consumption of the UAV assuming H_N as the optimized altitude given NOMA (detailed in Section V):

$$E_N = P_{max}(\frac{H_N}{v_{climb}}) + (\psi + \Gamma H_N)t. \tag{12}$$

Hence, the following difference equation can be used to compare the energy consumption of OMA and NOMA schemes:

$$E_O - E_N = \Delta E = (\Gamma t + \frac{P_{max}}{v_{climb}})\Delta h, \tag{13}$$

where $\Delta h = H_O - H_N$.

As Γ, P_{max}, t, *and* v can be considered constant values when UAVs with similar design specifications and velocity are deployed for both cases. $\Delta h > 0$ implies NOMA achieving better energy savings due to lower required altitude H_N.

IV. PERFORMANCE OF DOWNLINK ORTHOGONAL MULTIPLE ACCESS (OMA) AT THE OPTIMAL UAV ALTITUDE

In this section, the method of computing maximum sum-rate at the optimum UAV altitude for the proposed system model under OMA is discussed. The method assumes Time Division Multiple Access (TDMA) between two users, however, the concept can be easily extended to more number of users. This assumption brings OMA at par with NOMA for analysis purposes, considering the proposed scheme for 3GPP Long Term Evolution-Advanced (LTE-A), to group users by selecting two NOMA users within each group [30]. Later, the sum-rate and individual user-rates employing OMA are considered as bench marks and set as constraints in the study of NOMA viability of UAV-assisted communication systems. Assuming the system model, the channel between UAV-BS and the $j\,th$ user on the ground is denoted by $h_j = \frac{1}{\sqrt{1+\bar{L}_j(R_c,H)}}$ [31], where the small-scale fading effect is ignored as the channel model between the UAV and ground users is based on probabilistic LOS and NLOS links instead of the classical fading channel [19]. The channel capacity for any $user_j$ employing OMA is given as [32]:

$$R_j^{OMA} = \frac{1}{2}\log_2(1 + \gamma|h_j|^2),\ j \in \{r, s\}, \tag{14}$$

where γ and the constant factor $1/2$ represents the transmit Signal to Noise Ratio (SNR) and equal distribution of time resource between the two users, respectively. The sum-rate is given as:

$$C_{OMA} = \frac{1}{2}\log_2(1 + \gamma|h_r|^2) + \frac{1}{2}\log_2(1 + \gamma|h_s|^2). \tag{15}$$

As the channel capacity is a function of the channel gains, the next step is to find the optimal altitude for a given distribution of users. As presented in [7], assume a UAV-BS transmitting signals in the DL with a transmission power of P_{tx} then the mean received power at the $j\,th$ user can be written as:

$$P_{rx,j}(dB) = P_{tx} - \bar{L}(R_c, H). \tag{16}$$

The optimum altitude of UAV-BS, H_O with the minimum required transmission power can be calculated by solving [7]:

$$\frac{\partial P_{tx}}{\partial H} = \frac{\partial \bar{L}(R_c, H)}{\partial H} = 0. \tag{17}$$

Additionally, it is trivial to verify that the R_c as a function of H is a concave function and if a local maxima exists, then the corresponding value of altitude of UAV-BS, H_O becomes the global optimum. It is conceivable that for a given fixed coverage radius R_c, a UAV-BS at H_O provides the best possible SNR for all terrestrial users, which leads to maximized sum-rate [7]. Algorithm 1 provides the pseudo code to compute individual user-rate for OMA system. The algorithm utilizes MATLAB *fminsearch* function to find the optimal altitude of the UAV-BS that minimizes the path loss between the UAV and the cell-edge user. Once the optimal altitude H_O has been determined, individual user-rate for OMA is computed.

Algorithm 1 Maximum Sum-Rate for OMA

Input: $H, H_0, D_s, D_r, \aleph_{LOS}, \aleph_{NLOS}, \gamma, f_c, c, \alpha$, and β
Output: C_{OMA}^{max}

function main
  $[H_O, \overline{L_s}] \leftarrow$ fminsearch(FIT, H_0)
  $\overline{L_r} \leftarrow \Pr_r^{LOS} L_r^{LOS} + \Pr_r^{NLOS} L_r^{NLOS}$ ▷ (1)-(6)
  for $j \leftarrow r, s$ **do**
    $h_j \leftarrow \frac{1}{\sqrt{1+\overline{L_j}}}$
    $R_j^{OMA} \leftarrow \frac{1}{2}\log_2(1+\gamma|h_j|^2)$
  end for
  $C_{OMA}^{max} \leftarrow R_r^{OMA} + R_s^{OMA}$
  return C_{OMA}^{max}
end function

function Fit(H)
  $\overline{L_s} \leftarrow \Pr_s^{LOS} L_s^{LOS} + \Pr_s^{NLOS} L_s^{NLOS}$ ▷ (1)-(6)
  return $\overline{L_s}$
end function

V. PERFORMANCE OF DOWNLINK NON-ORTHOGONAL MULTIPLE ACCESS (NOMA)

In this section, the performance of the system under our considerations is maximized for the cases of capacity and coverage. An optimization problem for each case is formulated with minimum target rate, i.e. data rate achievable by OMA, being set as constraint. Three cases of the optimization are considered as follows:

1) Sum-rate maximization as a function of power allocation coefficients (Altitude fixed as in OMA)
2) Sum-rate maximization as a function of altitude of the UAV (Altitude optimized for NOMA)
3) Coverage maximization as a function of altitude of the UAV (Altitude optimized for NOMA)

A. ALTITUDE FIXED NOMA SUM-RATE MAXIMIZATION

As channel gain is a decreasing function of the distance between the transmitter and the receiver, it is evidently stated that $|h_s|^2 \leq |h_r|^2$ for the $s\,th$ and $r\,th$ user selected to utilize NOMA, $1 \leq s \leq r$. Considering DL NOMA, the channel capacity for $s\,th$ and $r\,th$ users are given, respectively as [32]:

$$R_s^{NOMA} = \log_2\left(1 + \frac{\omega_s|h_s|^2}{\omega_r|h_s|^2 + 1/\gamma}\right) \tag{18}$$

and

$$R_r^{NOMA} = \log_2(1 + \omega_r\gamma|h_r|^2), \tag{19}$$

where ω_s and ω_r represent the power allocation coefficients for users s and r, respectively and $\omega_s = 1 - \omega_r$. The necessary condition for user r to successfully remove $s\,th$ user interference before the $r\,th$ user can detect its own message, given by $R_{r\to s}^{NOMA} \geq R_s^{NOMA}$, is always satisfied for $|h_s|^2 \leq |h_r|^2$, where $R_{r\to s}^{NOMA} = \log_2(1+\frac{\omega_s|h_r|^2}{\omega_r|h_r|^2+1/\gamma})$ [33]. For NOMA that employs multiple access in the power domain, the potential gains can be achieved by allocating power to paired users based on instantaneous channel gains opposed to fixed power allocation scheme [12], [17], [32], which cannot always guarantee to meet Quality-of-Service (QoS) without thoughtfully adjusting various parameters [31], [33]. Additionally, the gains of NOMA can be weighed against OMA only if the data rates achieved by NOMA are strictly better or at least equal to data rates achievable by OMA schemes [32], [34]. Thus, the problem of sum-rate maximization can be written as an optimization problem:

$$\max_{\omega_s,\omega_r} C^{NOMA} \tag{20}$$

$$\text{subject to}: \ \text{constraint } 1: \ R_{r,H_O}^{NOMA} \geq R_{r,H_O}^{OMA} \tag{21}$$

$$\text{constraint } 2: \ R_{s,H_O}^{NOMA} \geq R_{s,H_O}^{OMA} \tag{22}$$

$$\text{constraint } 3: \ \omega_s + \omega_r \leq 1, \tag{23}$$

where $C^{NOMA} = R_s^{NOMA} + R_r^{NOMA}$. Here the first two constraints ensure that NOMA strictly guarantees better or equivalent individual rates compared to the ones achieved by OMA schemes. And the last constraint ensures the total transmitted power does not exceed the maximum allowed transmission power. Following the procedure for power allocation presented in [32], the user with higher channel gain is assumed to be the primary user. Thus, the lower bound of the power allocation factor w_r using the relationship defined by *constraint* 1 is given as:

$$\log_2(1 + \omega_r\gamma|h_r|^2) \geq \frac{1}{2}\log_2(1 + \gamma|h_r|^2). \tag{24}$$

Then,

$$\omega_r \geq \frac{1}{y+1}, \tag{25}$$

where $y = (1+\gamma|h_r|^2)^{1/2}$. Similarly, solving for *constraint* 2 by assuming weaker channel user as the primary user, the upper bound on ω_r is as follows:

$$\log_2\left(1 + \frac{\omega_s|h_s|^2}{\omega_r|h_s|^2 + 1/\gamma}\right) \geq \frac{1}{2}\log_2(1 + \gamma|h_s|^2) \tag{26}$$

and

$$\omega_r \leq \frac{1}{z+1}, \tag{27}$$

where $z = (1+\gamma|h_s|^2)^{1/2}$. The upper and lower bounds for ω_r can be combined by introducing two tuning coefficients μ_1 and μ_2 given as:

$$\omega_r = \frac{\mu_1}{y+1} + \frac{\mu_2}{z+1}, \tag{28}$$

where $\mu_1 = 1 - \mu_2$. Thus, *constraints* 1 and 2 can be met simultaneously for any value of μ_i. Furthermore, these can be tuned to achieve trade-offs between sum-rate maximization and fairness among users or to meet diversified QoS requirements such as for neighborhood area networks applications in smart grid communication networks [35]. By using (18) and (19), C^{NOMA} is given by

$$C^{NOMA} = \log_2(1+\omega_r\gamma|h_r|^2) + \log_2(1+\frac{\omega_s|h_s|^2}{\omega_r|h_s|^2+1/\gamma}). \tag{29}$$

Equivalently,

$$C^{NOMA} = \log_2(1+\omega_r\gamma|h_r|^2) + \log_2(\frac{1+\gamma|h_s|^2}{1+\omega_r\gamma|h_s|^2}). \tag{30}$$

It can be observed in (30) that $\omega_r\gamma|h_s|^2 < \omega_r\gamma|h_r|^2$ as $|h_s|^2 \leq |h_r|^2$, thus the sum-rate for NOMA monotonically increases with increasing ω_r. Furthermore, as ω_r is an increasing function of μ_2 and the maximum value of μ_2 i.e. 1, maximizes the sum-rate of NOMA.

The solution to the optimization problem defined by (20)-(23) is given by:

$$C^{NOMA}_{max} = \log_2(\frac{z^2+zy^2}{z+1}). \tag{31}$$

Algorithm 2 summarizes the methodology to maximize sum-rate for NOMA based UAV-BS through power allocation factor optimization. The method seeks to highlight the performance of NOMA by fixing altitude of the UAV to the same value acquired for OMA. The algorithm commences by determining the individual user-rate for OMA based UAV-BS, to be used as constraints by making use of *fminsearch* MATLAB function. Then, power allocation factor ω_r is computed using (28). Finally, the sum-rate is given by (31).

Algorithm 2 Maximum Sum-Rate for NOMA (Altitude Fixed)

Input: $H, H_0, D_s, D_r, \aleph_{LOS}, \aleph_{NLOS}, \gamma, f_c, c, \alpha$, and β
Output: C^{NOMA}_{max}

function main
  $[H_O, \overline{L_s}] \leftarrow$ fminsearch(FIT,H_0)
  $\overline{L_r} \leftarrow \Pr_r^{LOS} L_r^{LOS} + \Pr_r^{NLOS} L_r^{NLOS}$ ▷ (1)-(6)
  $h_r \leftarrow \frac{1}{\sqrt{1+\overline{L_r}}}$
  $h_s \leftarrow \frac{1}{\sqrt{1+\overline{L_s}}}$
  $\omega_r \leftarrow \frac{1}{1+\sqrt{1+\gamma|h_s|^2}}$
  $\omega_s \leftarrow 1 - \omega_r$
  $R_r^{NOMA} \leftarrow \log_2(1+\omega_r\gamma|h_r|^2)$
  $R_s^{NOMA} \leftarrow \log_2\left(1+\left[\frac{\omega_s|h_s|^2}{\omega_r|h_s|^2+\frac{1}{\gamma}}\right]\right)$
  $C^{NOMA}_{max} \leftarrow R_r^{NOMA} + R_s^{NOMA}$
  return C^{NOMA}_{max}
end function

function Fit(H)
  $\overline{L_s} \leftarrow \Pr_s^{LOS} L_s^{LOS} + \Pr_s^{NLOS} L_s^{NLOS}$ ▷ (1)-(6)
  return $\overline{L_s}$
end function

B. ALTITUDE OPTIMIZED NOMA SUM-RATE MAXIMIZATION

The maneuverability of a UAV-BS provides an extra degrees of freedom which can be utilized to achieve increased gains as compared to static BS nodes. By observing (30), it is easy to conclude that the effect of power allocation on sum-rate can be further enhanced by adjusting the channel gains between UAV-BS and the ground users through altitude optimization of the UAV-BS. According to (30), the sum-rate maximization is an increasing function of ω_r and the channel gain between UAV-BS. The ability to manipulate the channel gain is a particular virtue of the mobile UAV-BS, which cannot be realized in case of static BS. Moreover, the NOMA exhibits the best possible performance gains over OMA when the channel between NOMA pair has distinctive channel conditions [33], [34]. Two cases are considered to elaborate the effect of changing the altitude of the UAV-BS at the overall system performance:

1) Increasing altitude above the optimum altitude for OMA calculated in Section IV. In the proposed system, the constraints defined by (21) and (22) are computed by finding the optimum altitude based on minimum path loss between the cell-edge user and the UAV-BS. Increasing the altitude above this level has a negative impact on decreasing channel gains for both users. Moreover, the difference between channel gains of the ground users gradually reduces as the altitude of UAV-BS increases. The finding has been arisen by both increasing elevation angle and distance between the UAV-BS and the *r th* user. Thus, it is capable of reducing the overall sum-rate.
2) Decreasing the altitude below the optimum altitude for OMA calculated in Section IV. Reducing the altitude of the UAV-BS below the optimum altitude, i.e. moving the UAV-BS closer to the *r th* user has several benefits. More explicitly, reducing altitude improves the channel gain between the *r th* user and the UAV-BS due to reduced distance. Based on the channel model for the system model and observing the first term in (30), no improvement in the sum-rate can be achieved as the cell-edge user has the optimum channel gain at the optimum altitude. On the other hand, the second term in (30) $\log_2(1+\omega_r\gamma|h_r|^2)$, can bring in further improvement in the overall sum-rate by finding the

optimum UAV-BS altitude for the maximum sum-rate. Simultaneously, the channel gain between the UAV-BS and the cell-edge user degrades as it deviates from the optimum altitude. This results in pairing between users with distinctive channel characteristics. More specifically, the best possible pair may be a set of two users experiencing the best and worst channels, respectively. The best channel user paired with worst channel user, which leads to reducing power being utilized to meet QoS of the user having higher channel gain and the remaining power is available to the user with lower channel gain. Note that, the altitude is one of the major factors affecting the energy efficiency of the UAV based on (10). Thus, a reduction in operating altitude of the UAV-BS results in a favorable outcome for the proposed system.

As discussed, the maximum sum-rate for NOMA based UAV-BS is a function of both channel gain and power allocation, ω_r to the strong channel user, where the channel gain is a function of altitude of the UAV-BS, H. The optimization problem expressed in (20)-(23) can be re-written as:

$$\max_{H} C^{NOMA} \tag{32}$$

$$subject\ to: \quad constraint\ 1: \ R^{NOMA}_{r,H_N} \geq R^{OMA}_{r,H_O} \tag{33}$$

$$constraint\ 2: \ R^{NOMA}_{s,H_N} \geq R^{OMA}_{s,H_O} \tag{34}$$

$$constraint\ 3: \ \omega^{min}_{s,H_N} + \omega^{min}_{r,H_N} \leq 1, \tag{35}$$

where *constraints* 1 and 2 set lower bound on user-rates for NOMA while *constraint* 3 defines the feasible range of solutions for the above-defined problem. It should be noted that a feasible solution in the context of this paper is an altitude of UAV-BS for which both *constraints* 1 and 2 can be simultaneously satisfied within limits of the maximum allowed transmission power.

Considering the r *th* user as the primary user, the lower bound for ω_{r,H_N} is given as:

$$\log_2(1 + \omega_{r,H_N}\gamma|h_{r,H_N}|^2) \geq R^{OMA}_{r,H_O}. \tag{36}$$

Then,

$$\omega_{r,H_N} \geq \frac{\varepsilon_r - 1}{G_r}, \tag{37}$$

where $\varepsilon_r = 2^{R^{OMA}_{r,HO}}$ and $G_r = \gamma|h_{r,H_N}|^2$. Similarly, considering s *th* user as the primary user, the upper bound for ω_{r,H_N} is given by:

$$\log_2(1 + \frac{\omega_{s,H_N}|h_{s,H_N}|^2}{\omega_{r,H_N}|h_{s,H_N}|^2 + 1/\gamma}) \geq R^{OMA}_{s,H_O}. \tag{38}$$

Then,

$$\omega_{r,H_N} \leq \frac{1 - \varepsilon_s + G_s}{\varepsilon_s G_s}, \tag{39}$$

where $\varepsilon_s = 2^{R^{OMA}_{s,HO}}$ and $G_s = \gamma|h_{s,H_N}|^2$ The upper and lower bounds for ω_{r,H_N} can be combined as:

$$\omega_{r,H_N} = \frac{\mu_1(\varepsilon_r - 1)}{G_r} + \frac{\mu_2(1 - \varepsilon_s + G_s)}{\varepsilon_s G_S}. \tag{40}$$

Algorithm 3 Maximum Sum-Rate for NOMA (Altitude Optimized)

Input: H_0,D_s,D_r,R^{OMA}_s,R^{OMA}_s,$\aleph_{LOS}$, $\aleph_{NLOS}$,lb,ub,γ,f_c,c,α,and β
Output: C^{NOMA}_{max}

function main
  $[H_N, C^{NOMA}] \leftarrow$ fmincon(FIT,H_0,lb,ub,CONSTRT)
  $C^{NOMA}_{max} \leftarrow -C^{NOMA}$
  return C^{NOMA}_{max}
end function

function Fit(H)
  for $j \leftarrow r, s$ **do**
    $\overline{L_j} \leftarrow \Pr^{LOS}_j L^{LOS}_j + \Pr^{NLOS}_j L^{NLOS}_j$ ▷ (1)-(6)
    $h_j \leftarrow \frac{1}{\sqrt{1+L_j}}$
  end for
  $\varepsilon_s \leftarrow 2^{R^{OMA}_s}$
  $G_s \leftarrow \gamma|h_s|^2$
  $\omega_r \leftarrow \frac{1-\varepsilon_s+G_s}{\varepsilon_s G_s}$
  $\omega_s \leftarrow 1 - \omega_r$
  $R^{NOMA}_r \leftarrow \log_2(1 + \omega_r\gamma|h_r|^2)$
  $R^{NOMA}_s \leftarrow \log_2(1 + \left[\frac{\omega_s|h_s|^2}{\omega_r|h_s|^2+\frac{1}{\gamma}}\right])$
  $C^{NOMA} \leftarrow -(R^{NOMA}_r + R^{NOMA}_s)$
  return C^{NOMA}
end function

function Constrt(H)
  for $j \leftarrow r, s$ **do**
    $\overline{L_j} \leftarrow \Pr^{LOS}_j L^{LOS}_j + \Pr^{NLOS}_j L^{NLOS}_j$ ▷ (1)-(6)
    $h_j \leftarrow \frac{1}{\sqrt{1+L_j}}$
  end for
  $\varepsilon_r \leftarrow 2^{R^{OMA}_r}$
  $\varepsilon_s \leftarrow 2^{R^{OMA}_s}$
  $G_r \leftarrow \gamma|h_r|^2$
  $G_s \leftarrow \gamma|h_s|^2$
  $\omega^{min}_r \leftarrow \frac{\varepsilon_r - 1}{G_r}$
  $\omega^{min}_s \leftarrow 1 - \left[\frac{1-\varepsilon_s+G_s}{\varepsilon_s G_s}\right]$
  $cineq \leftarrow \left[\omega^{min}_r + \omega^{min}_s - 1\right]$
  return $cineq$
end function

The maximum sum-rate is achieved for $\mu_2 = 1$, i.e.

$$\omega_{r,H_N} = \frac{1 - \varepsilon_s + G_s}{\varepsilon_s G_s}, \tag{41}$$

where $\omega_{s,H_N} = 1 - \omega_{r,H_N}$. The problem of finding the optimal altitude for maximizing the sum-rate is solved using interior point method [36]. Algorithm 3 illustrates pseudo code of the proposed methodology. The sum-rate is maximized as a function of altitude of the UAV-BS. Similarly, the optimum value of H_O is computed using *fminsearch* function of MATLAB.

C. ALTITUDE OPTIMIZED NOMA COVERAGE MAXIMIZATION

The channel capacity gains of NOMA over OMA can be translated into larger footprint for the aerial cell. The basic idea is to maximize the data rate for the cell-edge user, which is then utilized to extend the coverage ability of the UAV further. It should be noted that the coverage extension is performed keeping in view the minimum performance threshold. Let C defines the circular coverage area of the aerial cell. Then, the coverage maximization problem can be posed as:

$$\max_{H,D_s} \mathsf{C} \tag{42}$$

$$subject\ to: \quad constraint\ 1 \ : R_{j,H_N}^{NOMA} \geq R_{th}\,,\ j \in \{r, s\}, \tag{43}$$

$$constraint\ 2 \ : \omega_{s,H_N}^{min} + \omega_{r,H_N}^{min} \leq 1, \tag{44}$$

where D_s corresponds to the maximum distance from an aerial-cell center to the cell-edge user (Fig. 1) defining the radius of the aerial cell (R_c), H_N defines the optimized UAV altitude assuming NOMA, and R_{th} represents the user-rate threshold. The maximization problem requires finding the maximum distance D_s and the corresponding optimized UAV altitude for which the minimum rate threshold can be met. The optimization problem is solved by decoupling the problem into vertical and horizontal optimizations, which are solved iteratively [37]. Given a minimum rate threshold and the corresponding maximum coverage radius assuming OMA, the first step involves UAV altitude optimization such that the rate for the cell-edge user is maximized while meeting the rate constraints for both users. The cell-center user is allocated power which is just enough to meet the rate threshold by setting $\omega_{r,H_N} = \frac{\varepsilon_r - 1}{G_r}$ in (41), whereas the cell-edge user is allocated with all of the remaining power ($\omega_{s,H_N} = 1 - \omega_{r,H_N}$), thus achieving the desired rate maximization. The horizontal optimization is facilitated by the optimized altitude and the maximized cell-edge user rate or equivalently the surplus power to widen the coverage area of the aerial cell.

VI. SIMULATION AND RESULTS

The simulations have been performed assuming urban, sub-urban and dense-urban environments with $\eta = 2$ for free-space path loss. Referring to Fig. 1, the distance of the $r\,th$ user for all simulations is given as $D_r = 20\ m$, whereas the distance of $s\,th$ cell-edge user, $D_s \in \{60, 120, 180\}\ m$, to study the effect of increasing coverage area on the performance of the proposed system. The parameters for the considered environment are listed in table 1 (unless otherwise stated) [23].

TABLE 1. Simulation parameters for the considered environment.

Parameters	Sub-urban	Urban	Dense-urban
α	4.8860	9.6177	12.0870
β	0.4290	0.1581	0.1139
$\varkappa_{LOS}$	0.1	1	1.6
$\varkappa_{NLOS}$	21	20	23

Fig. 3 illustrates the sum-rate of two cases of NOMA for changing coverage regions at transmit SNRs of 15 dB and 25 dB. The higher sum-rate gain in comparison with OMA and altitude fixed NOMA highlights the efficacy of the proposed altitude optimization. Though the fixed altitude NOMA conforms to the set constraints. The altitude optimization creates more substantial channel gain difference for the two users manifesting the best possible pairing between two users experiencing the best and worst channels, respectively. Thus, the proposed altitude optimization generates a more conducive environment for NOMA yielding greater gains overall. At higher SNR regime, the altitude optimized NOMA is considerably better than both the altitude fixed OMA and NOMA.

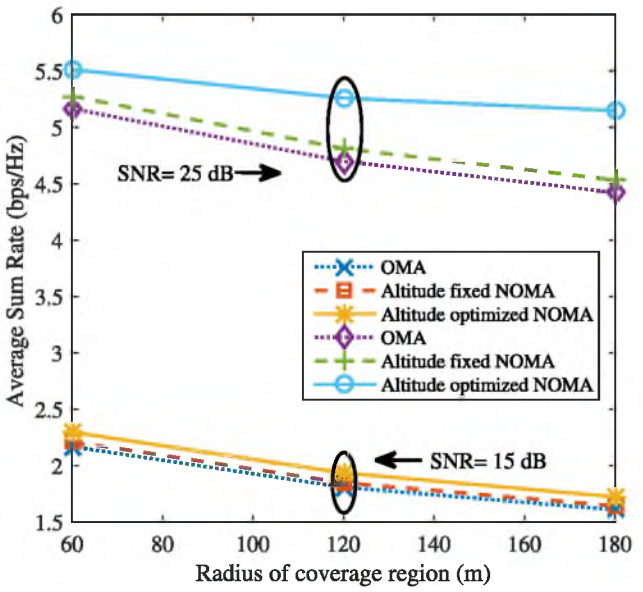

FIGURE 3. NOMA capacity performance comparison between altitude optimized and altitude fixed schemes in an urban environment.

Fig. 4 depicts plots of energy efficiency parameter Δh that are compared for sub-urban, urban, and dense-urban environments against increasing SNR values. As energy consumption of the UAV-BS is an increasing function of its altitude, increasing Δh represents the increasing energy efficiency of NOMA compared to OMA. The higher probability of NLOS links for some users in the dense-urban environment causes larger difference between user channel gains. This results in much larger energy gain for dense-urban areas than to those for other areas, which is attributed to better NOMA gains for a user pair exhibiting the best and worst channel conditions.

The energy efficiency of the proposed scheme is further clarified by comparing UAV energy consumption between OMA and NOMA as portrayed in Fig. 5. The energy consumption of the UAV is computed using (10) and (11), where ψ, Γ, t, P_{max}, and v are set as 30, 10.5, 1200 *second*, 85 *watt*, and 2 *m/s*, respectively [29]. The lower required altitude to cover a given sub-urban area as compared to urban and dense-urban allows achieving higher energy efficiency.

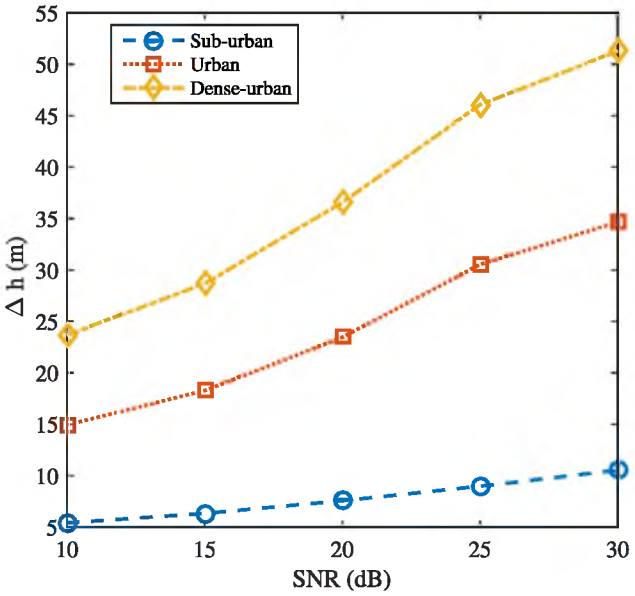

FIGURE 4. Δh: Altitude optimized NOMA energy performance parameter for different environments with $R_C = 60$ *m*.

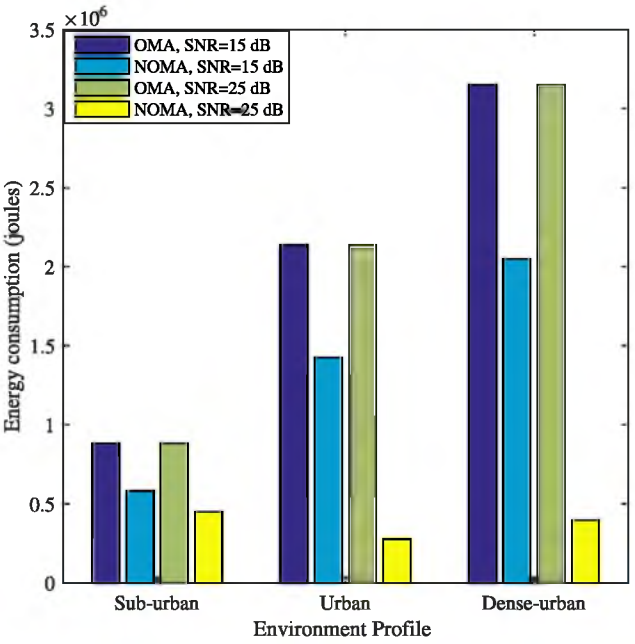

FIGURE 5. Energy consumption of UAV: OMA versus NOMA for $R_c = 180$ *m*.

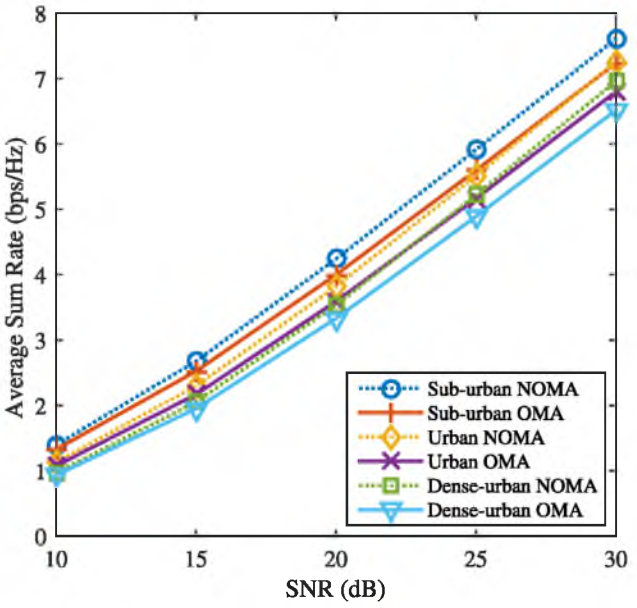

FIGURE 6. Average sum-rate at various environments for $R_c = 60$ *m*.

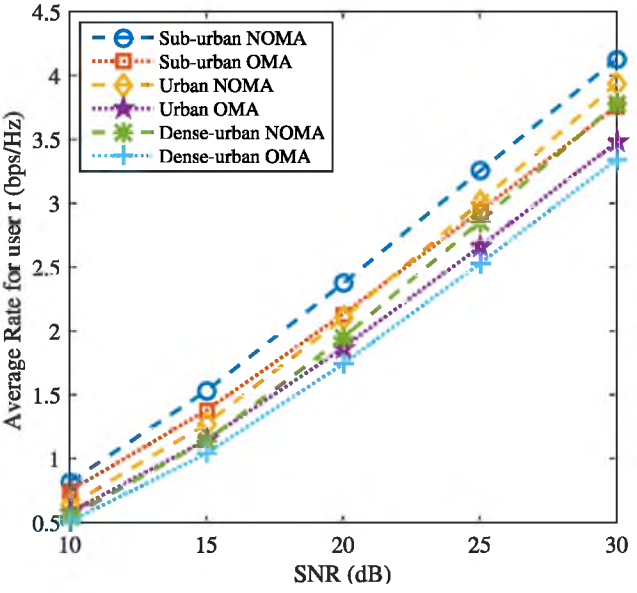

FIGURE 7. Average rate for user r for $R_c = 60$ *m*.

On the other hand, the lower distinction between user channels as in the case of a sub-urban environment profile generates lesser disparity between the rate constraints and corresponding power allocation between the cell-center and the cell-edge users, thus affecting the overall gain of NOMA over OMA.

Figs. 6, 7, and 8 provide a comparative analysis of the proposed solution to the optimization problem defined by (32)-(35) for urban, sub-urban, and dense-urban environments with the radius of coverage area fixed at 60 m. Fig. 6 demonstrates NOMA manifesting better performance in terms of spectral efficiency while simultaneously meeting the constraints as elaborated in Figs. 7 and 8. It can be observed in Fig. 7 that the average rate for the stronger user ($r\,th$) is always better than the rate realized by OMA as μ_2 is set unity in (40), whereas Fig. 8 shows that the weaker user ($s\,th$) achieves the same rate as realized for OMA scheme. This allows the users with the better channel, $r\,th$ user to contribute more towards increasing the sum-rate of the system.

The distinctive channel conditions of the two users and high SNR collectively exploit NOMA for better gains.

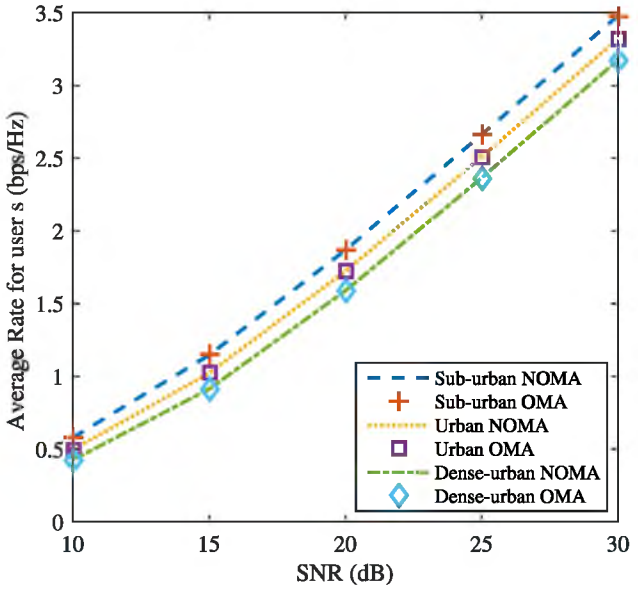

FIGURE 8. Average rate for user s for $R_c = 60$ m.

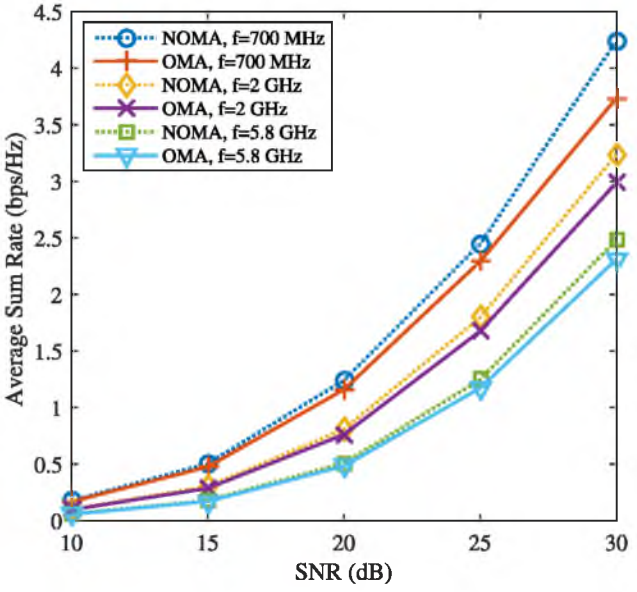

FIGURE 10. Average sum-rate: Altitude optimized NOMA with different carrier frequencies for dense-urban environment with $R_c = 120$ m.

The proposed altitude optimization further enhances this remarkable feature of NOMA. As depicted in Fig. 9, this unique feature of NOMA, in contrast to OMA, allows expanding the coverage area without sacrificing achievable sum-rates substantially.

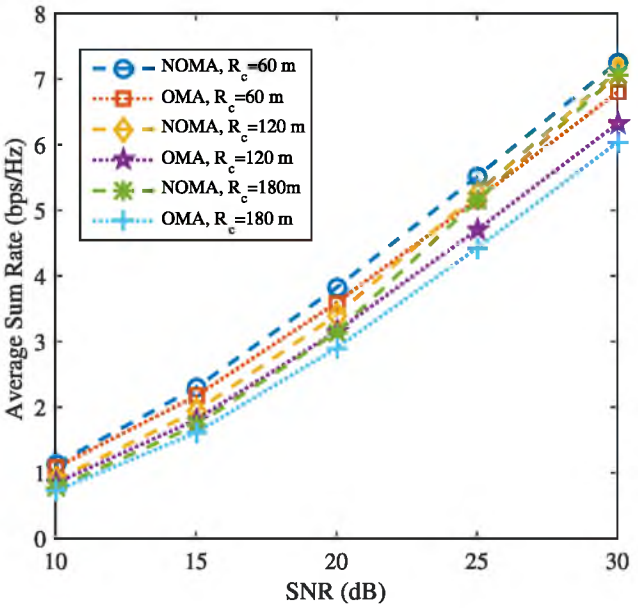

FIGURE 9. Average sum-rate: Altitude optimized NOMA with different target regions in an urban environment.

The investigated effect of three sub-6 GHz carrier frequencies on the performance of the proposed scheme is illustrated in Fig. 10. The results are computed using the free-space path loss formula $20\log(\frac{4\pi f_{cX_j}}{c})$ in (7), where c is the speed of light [7]. The values of $(\varkappa_{LOS}, \varkappa_{NLOS})$ for dense-urban environment are taken as (1, 20), (1.6, 23), and (1.8, 26)

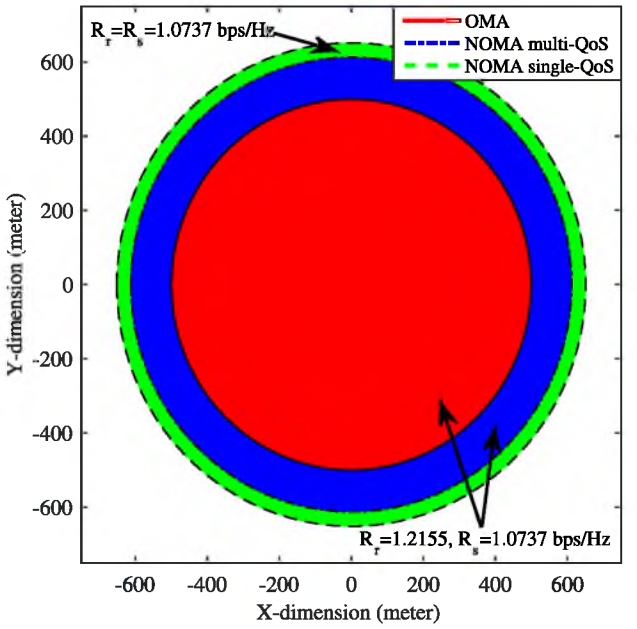

FIGURE 11. Coverage comparison for a given target rate: OMA versus NOMA for urban environment at $SNR = 20$ dB.

for 700 MHz, 2 GHz, and 5.8 GHz carrier frequencies (f_c), respectively [23]. The results highlight the dependency of the anticipated performance gains of NOMA over OMA in terms of the achievable sum-rate on the selection of the carrier frequency. According to the findings, NOMA's sum-rate gain over OMA is a decreasing function of the carrier frequency.

The demonstrated NOMA's rate gains against OMA can be translated into wider coverage as manifested in Fig. 11. The performance of coverage maximization method for NOMA assisted UAV communication system presented

in Section V is studied for a single minimum QoS as well as multiple QoS thresholds. The red disk area in the Fig. 11 represents a maximum coverage radius of 500 m for OMA UAV communication system, where 1.2155 bps/Hz and 1.0737 bps/Hz are the maximum rates for the user at the cell-center and the cell-edge, respectively. Considering these maximum possible rates for the two users as constraints, NOMA is capable of guaranteeing a coverage expansion by 22.50 % (blue disk) over OMA.

The multiple QoS scheme provides a fair benchmark for the analysis between the OMA and NOMA. However, it is worthy to highlight that the maximum possible coverage of UAV communication systems is conventionally designed assuming a user as having data rates greater or equal to a single minimum QoS threshold in the literature [6], [20]. Following a similar approach, the proposed scheme enables the coverage area to be enhanced by a total of 30.31 % (green disk) over OMA (red disk) assuming a minimum limit of 1.0737 bps/Hz for all users. Thus, depicting a significant advantage of NOMA over OMA.

VII. CONCLUSION

This paper investigated an account of NOMA's applicability for UAV-assisted communication systems. The crucial need to transmit more bits per joule inspired the proposed scheme for sum-rate maximization with reduced energy consumption. Taken together, presented results manifests that NOMA performs better than OMA while fulfilling individual user-rate constraint for both users. In addition to the spectral efficiency, the reduction in the UAV altitude as compared to OMA brings in the most needed energy efficiency for the proposed scheme. A useful feature of our proposed scheme allows the expansion of the coverage region without incurring substantial loss of the sum-rate. This feature is of most importance for dense-urban catastrophic situations providing coverage to larger areas utilizing fewer UAVs. Moreover, the scheme provides flexibility for precise UAV altitude adjustment at the expense of reduced sum-rate, as a consequence of the range of possible altitudes for which the individual user-rate constraint can be satisfied. It is also noted that the employment of lower carrier frequency leads to better NOMA's sum-rate gain. In the future, power allocation scheme for both multi-cell and multi-UAV communication scenarios can be formulated along with the study of user-pairing algorithms.

REFERENCES

[1] A. M. Hayajneh, S. A. R. Zaidi, D. C. McLernon, and M. Ghogho, "Drone empowered small cellular disaster recovery networks for resilient smart cities," in *Proc. IEEE Int. Conf. Sens., Commun. Netw. (SECON Workshops)*, Jun. 2016, pp. 1–6.

[2] I. Bor-Yaliniz and H. Yanikomeroglu, "The new frontier in RAN heterogeneity: Multi-tier drone-cells," *IEEE Commun. Mag.*, vol. 54, no. 11, pp. 48–55, Nov. 2016.

[3] Y. Zeng *et al.*, "Throughput maximization for UAV-enabled mobile relaying systems," *IEEE Trans. Commun.*, vol. 64, no. 12, pp. 4983–4996, Dec. 2016.

[4] S. Chandrasekharan *et al.*, "Designing and implementing future aerial communication networks," *IEEE Commun. Mag.*, vol. 54, no. 5, pp. 26–34, May 2016.

[5] R. I. Bor-Yaliniz, A. El-Keyi, and H. Yanikomeroglu, "Efficient 3-D placement of an aerial base station in next generation cellular networks," in *Proc. IEEE Int. Conf. Commun. (ICC)*, May 2016, pp. 1–5.

[6] M. Mozaffari, W. Saad, M. Bennis, and M. Debbah, "Efficient deployment of multiple unmanned aerial vehicles for optimal wireless coverage," *IEEE Commun. Lett.*, vol. 20, no. 8, pp. 1647–1650, Aug. 2016.

[7] M. Mozaffari, W. Saad, M. Bennis, and M. Debbah, "Drone small cells in the clouds: Design, deployment and performance analysis," in *Proc. IEEE Global Commun. Conf. (GLOBECOM)*, Dec. 2015, pp. 1–6.

[8] Y. Zeng, R. Zhang, and T. J. Lim, "Wireless communications with unmanned aerial vehicles: Opportunities and challenges," *IEEE Commun. Mag.*, vol. 54, no. 5, pp. 36–42, May 2016.

[9] S. Ali, E. Hossain, and D. I. Kim, "Non-orthogonal multiple access (NOMA) for downlink multiuser MIMO systems: User clustering, beamforming, and power allocation," *IEEE Access*, vol. 5, pp. 565–577, Mar. 2017.

[10] Y. Sun, D. W. K. Ng, Z. Ding, and R. Schober, "Optimal joint power and subcarrier allocation for full-duplex multicarrier non-orthogonal multiple access systems," *IEEE Trans. Commun.*, vol. 65, no. 3, pp. 1077–1091, Mar. 2017.

[11] S. M. R. Islam, N. Avazov, O. A. Dobre, and K.-S. Kwak, "Power-domain non-orthogonal multiple access (NOMA) in 5G systems: Potentials and challenges," *IEEE Commun. Surveys Tuts.*, vol. 19, no. 2, pp. 721–742, 2nd Quart., 2017.

[12] Z. Ding *et al.*, "Application of non-orthogonal multiple access in LTE and 5G networks," *IEEE Commun. Mag.*, vol. 55, no. 2, pp. 185–191, Feb. 2017.

[13] S. Lee, D. B. da Costa, Q.-T. Vien, T. Q. Duong, and R. T. de Sousa, "Non-orthogonal multiple access schemes with partial relay selection," *IET Commun.*, vol. 11, no. 6, pp. 846–854, 2017.

[14] Z. Yang, Z. Ding, P. Fan, and N. Al-Dhahir, "The impact of power allocation on cooperative non-orthogonal multiple access networks with SWIPT," *IEEE Trans. Wireless Commun.*, vol. 16, no. 7, pp. 4332–4343, Jul. 2017.

[15] Z. Chen, Z. Ding, X. Dai, and R. Zhang, "An optimization perspective of the superiority of noma compared to conventional OMA," *IEEE Trans. Signal Process.*, vol. 65, no. 19, pp. 5191–5202, Oct. 2017.

[16] P. Xu and K. Cumanan, "Optimal power allocation scheme for non-orthogonal multiple access with α-fairness," *IEEE J. Sel. Areas Commun.*, vol. 35, no. 10, pp. 2357–2369, Oct. 2017.

[17] M. S. Ali, H. Tabassum, and E. Hossain, "Dynamic user clustering and power allocation for uplink and downlink non-orthogonal multiple access (NOMA) systems," *IEEE Access*, vol. 4, pp. 6325–6343, 2016.

[18] Z. Chen, Z. Ding, and X. Dai, "Beamforming for combating inter-cluster and intra-cluster interference in hybrid NOMA systems," *IEEE Access*, vol. 4, pp. 4452–4463, Aug. 2016.

[19] M. Mozaffari, W. Saad, M. Bennis, and M. Debbah, "Unmanned aerial vehicle with underlaid device-to-device communications: Performance and tradeoffs," *IEEE Trans. Wireless Commun.*, vol. 15, no. 6, pp. 3949–3963, Jun. 2016.

[20] A. Al-Hourani, S. Kandeepan, and S. Lardner, "Optimal LAP altitude for maximum coverage," *IEEE Wireless Commun. Lett.*, vol. 3, no. 6, pp. 569–572, Dec. 2014.

[21] P. K. Sharma and D. I. Kim, "UAV-enabled downlink wireless system with non-orthogonal multiple access," in *Proc. IEEE Globecom Workshops (GC Wkshps)*, Dec. 2017, pp. 1–6.

[22] S. Jeong, O. Simeone, and J. Kang, "Mobile edge computing via a UAV-mounted cloudlet: Optimization of bit allocation and path planning," *IEEE Trans. Veh. Technol.*, vol. 67, no. 3, pp. 2049–2063, Mar. 2018.

[23] A. Al-Hourani, S. Kandeepan, and A. Jamalipour, "Modeling air-to-ground path loss for low altitude platforms in urban environments," in *Proc. IEEE Global Commun. Conf. (GLOBECOM)*, Dec. 2014, pp. 2898–2904.

[24] Q. Feng, J. McGeehan, E. K. Tameh, and A. R. Nix, "Path loss models for air-to-ground radio channels in urban environments," in *Proc. IEEE 63rd Veh. Technol. Conf.*, vol. 6. May 2006, pp. 2901–2905.

[25] D. Zorbas, T. Razafindralambo, D. P. P. Luigi, and F. Guerriero, "Energy efficient mobile target tracking using flying drones," *Proc. Comput. Sci.*, vol. 19, pp. 80–87, Jun. 2013.

[26] Y. Zhou, N. Cheng, N. Lu, and X. S. Shen, "Multi-UAV-aided networks: Aerial-ground cooperative vehicular networking architecture," *IEEE Veh. Technol. Mag.*, vol. 10, no. 4, pp. 36–44, Dec. 2015.
[27] J. Ueyama *et al.*, "Exploiting the use of unmanned aerial vehicles to provide resilience in wireless sensor networks," *IEEE Commun. Mag.*, vol. 52, no. 12, pp. 81–87, Dec. 2014.
[28] C. Di Franco and G. Buttazzo, "Energy-aware coverage path planning of UAVs," in *Proc. IEEE ICARSC*, Apr. 2015, pp. 111–117.
[29] D. Zorbas, L. Di Puglia Pugliese, T. Razafindralambo, and F. Guerriero, "Optimal drone placement and cost-efficient target coverage," *J. Netw. Comput. Appl.*, vol. 75, pp. 16–31, Nov. 2016.
[30] H. Lee, S. Kim, and J.-H. Lim, "Multiuser superposition transmission (MUST) for LTE-A systems," in *Proc. IEEE Int. Conf. Commun. (ICC)*, May 2016, pp. 1–6.
[31] Z. Ding, Z. Yang, P. Fan, and H. V. Poor, "On the performance of non-orthogonal multiple access in 5G systems with randomly deployed users," *IEEE Signal Process. Lett.*, vol. 21, no. 12, pp. 1501–1505, Dec. 2014.
[32] Z. Yang, Z. Ding, P. Fan, and N. Al-Dhahir, "A general power allocation scheme to guarantee quality of service in downlink and uplink NOMA systems," *IEEE Trans. Wireless Commun.*, vol. 15, no. 11, pp. 7244–7257, Nov. 2016.
[33] Z. Ding *et al.*, "Impact of user pairing on 5G nonorthogonal multiple-access downlink transmissions," *IEEE Trans. Veh. Technol.*, vol. 65, no. 8, pp. 6010–6023, Aug. 2016.
[34] Z. Ding, F. Adachi, and H. V. Poor, "The application of MIMO to non-orthogonal multiple access," *IEEE Trans. Wireless Commun.*, vol. 15, no. 1, pp. 537–552, Jan. 2016.
[35] S. Alam, M. F. Sohail, S. A. Ghauri, I. M. Qureshi, and N. Aqdas, "Cognitive radio based smart grid communication network," *Renew. Sustain. Energy Rev.*, vol. 72, pp. 535–548, May 2017.
[36] R. H. Byrd, M E. Hribar, and J. Nocedal, "An interior point algorithm for large-scale nonlinear programming," *SIAM J. Optim.*, vol. 9, no. 4, pp. 877–900, 1999.
[37] M. Alzenad, A. El-Keyi, F. Lagum, and H. Yanikomeroglu, "3-D Placement of an unmanned aerial vehicle base station (UAV-BS) for energy-efficient maximal coverage," *IEEE Wireless Commun. Lett.*, vol. 6, no. 4, pp. 434–437, Aug. 2017.

MUHAMMAD FARHAN SOHAIL (SM'17) received the B.S. degree in electronics engineering from International Islamic University, Islamabad, Pakistan, in 2007, and the M.S. degree in telecommunication engineering from the University of Melbourne, Australia, in 2008. He is currently pursuing the Ph.D. degree in electrical engineering with Universiti Teknologi Malaysia, Johor Bahru, Malaysia. Since 2009, he has been a Faculty Member with the Department of Electrical Engineering, National University of Modern Languages, Islamabad. His research interests include evolutionary computing techniques, MIMO, unmanned aerial vehicle-assisted mobile communication system, smart grid communication, and non-orthogonal multiple access.

CHEE YEN LEOW (S'08–M'12) received the B.Eng. degree in computer engineering from Universiti Teknologi Malaysia (UTM), Johor, Malaysia, and the Ph.D. degree from Imperial College London, London, U.K., in 2007 and 2011, respectively. Since 2007, he has been an Academic Staff with the Faculty of Electrical Engineering, UTM. He is currently a Senior Lecturer with the Faculty and a Research Fellow with the Wireless Communication Centre, Higher Institution Centre of Excellence, and UTM-Ericsson Innovation Centre for 5G. His research interests include cooperative communication, MIMO, drone communication, physical layer security, convex optimization, communications theory, wireless power transfer and communication, non-orthogonal multiple access, and 5G.

SEUNGHWAN WON (SM'16) received the B.S. and M.S. degrees in radio science and engineering from Korea University, Seoul, South Korea, in 1999 and 2001, respectively, and the Ph.D. degree from the Communications Research Group, School of Electronics and Computer Science, University of Southampton, U.K., in 2008 He was a Research Engineer with the Mobile Communication Technology Research Laboratory, LG Electronics R&D, from 2001 to 2004. He was a recipient of the 2004 State Scholarship of the Information and Telecommunication National Scholarship Program, Ministry of Information and Communication, South Korea.. His major research interests include synchronization and multi-user MIMO in mmW mobile communications, intelligent Internet of Thing, and intelligent Unmanned aerial vehicle-assisted mobile communication system. He published a host of papers in these research fields and secured more than 20 U.S. patents. Upon completing his Ph.D. degree, he returned to his native Korea and joined Samsung. In 2013, he was appointed as an Associate Professor by the University of Southampton. He is currently teaching and conducting research at the University of Southampton, Johor, Malaysia.